unbound concentrations in the liver estimated by the plasma concentration and protein binding. Since the protein binding of each psychotropic drug in tissues has not been reported, we assumed that these are the same as the protein binding in plasma.

Results

Inhibition of mexiletine p-*hydroxylase activity in human liver microsomes by psychotropic drugs*

The major metabolic pathways of mexiletine in humans are aromatic hydroxylation, forming *p*-hydroxymexiletine and aliphatic hydroxylation, forming 2-hydroxymexiletine. We previously reported that the kinetics and the contribution ratio of CYP2D6/CYP1A2 for *p*-hydroxylation and 2-hydroxylation are almost the same (Nakajima et al. 1998), i.e. the K_m values for mexiletine *p*-hydroxylation in recombinant CYP2D6 and CYP1A2 were 22.6 and 13.9 μM, respectively; the V_{max} values for mexiletine *p*-hydroxylation in CYP2D6 and CYP1A2 were 2249 and 4.7 fmol min^{-1} $pmol^{-1}$ CYP, respectively; the K_m values for mexiletine 2-hydroxylation in recombinant CYP2D6 and CYP1A2 were 22.1 and 15.2 μM, respectively; the V_{max} values for mexiletine 2-hydroxylation in CYP2D6 and CYP1A2 were 2492 and 6.1 fmol min^{-1} $pmol^{-1}$ CYP, respectively. Since *p*-hydroxymexiletine is more easily detected than 2-hydroxymexiletine with HPLC because of the higher absorbance coefficient, mexiletine *p*-hydroxylation in human liver microsomes was monitored in the present study.

The psychotropic drugs (100 μM) were screened for the inhibitory effects on mexiletine *p*-hydroxylase activity at a 10 μM mexiletine concentration (lower than K_m). As shown in Figure 2, mexiletine *p*-hydroxylase activity was completely abolished by paroxetine and thioridazine. In addition, 100 μM fluoxetine (17% of control), sertraline (12%) and desipramine (16%) extensively inhibited mexiletine *p*-hydroxylase activity. The IC_{50} values were 0.5 μM for paroxetine, 0.6 μM for thioridazine, 1.0 μM for fluoxetine, 11.0 μM for sertraline and 5.4 μM for desipramine (data not shown).

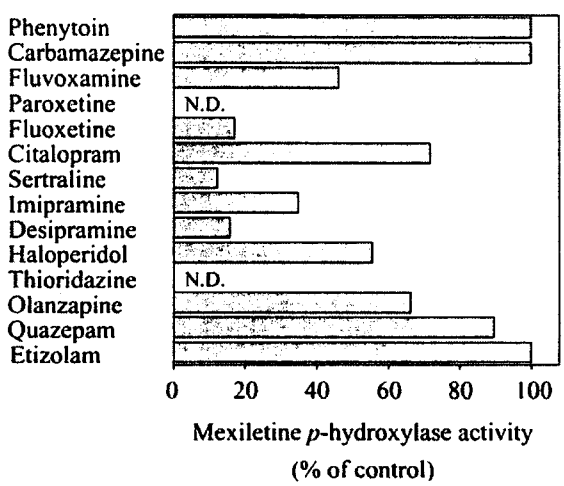

Figure 2. Inhibitory effects of psychotropic drugs on mexiletine *p*-hydroxylase activity in human liver microsomes. The concentrations of mexiletine and each psychotropic drug were 10 and 100 μM, respectively. Each column is the average of duplicate determinations. The control activity in the pooled human liver microsomes was 2.6 pmol min^{-1} mg^{-1} protein. N.D., not detected.

Inhibition constant and inhibition pattern

We determined the inhibition constants (K_i) for the compounds that exhibited extensive inhibition (Figure 3). The K_{is} and K_{ii} values are inhibition constants on the slope (competitive) and on the intercept (non-competitive), respectively. Paroxetine exhibited

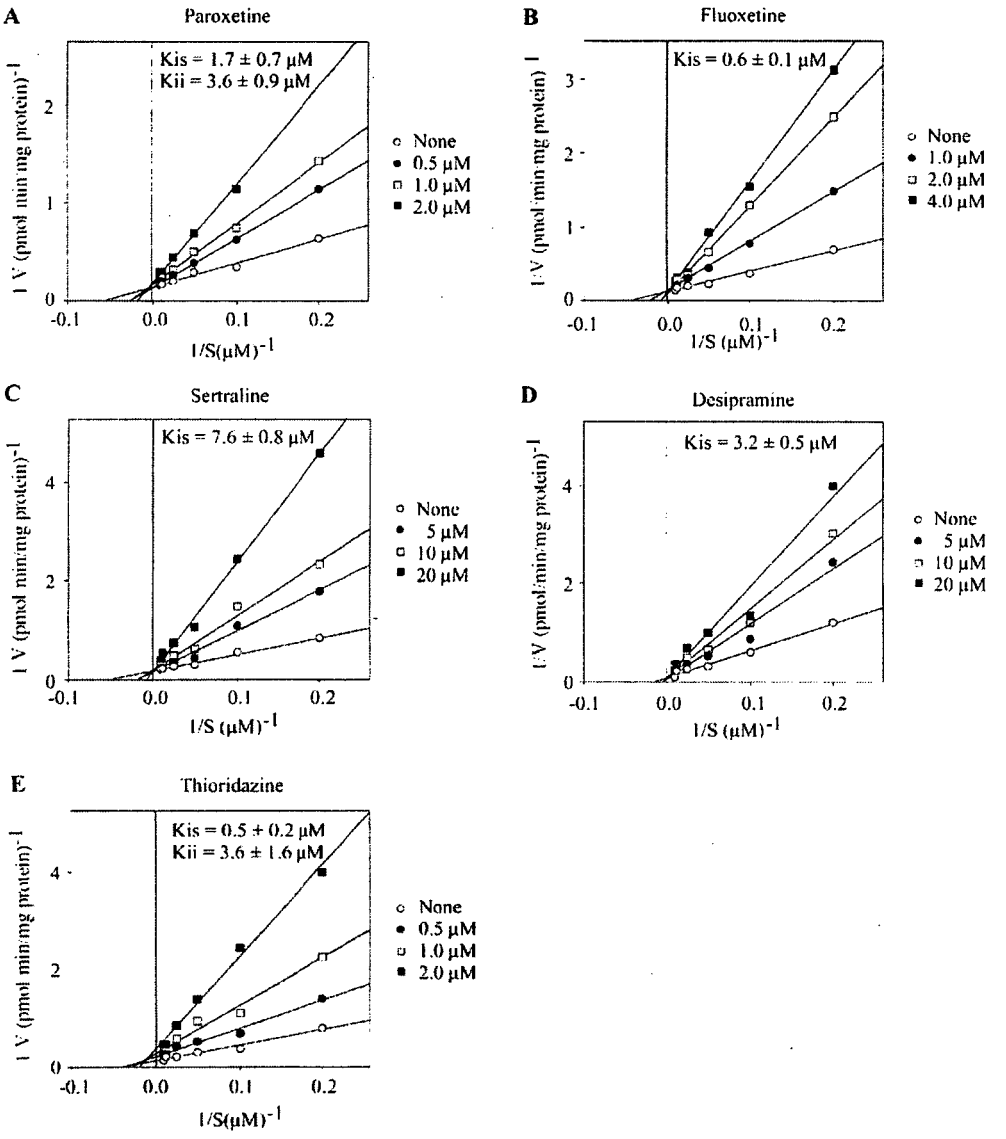

Figure 3. Lineweaver–Burk plots of mexiletine *p*-hydroxylase activity in human liver microsomes. Effects of (A) paroxetine, (B) fluoxetine, (C) sertraline, (D) desipramine and (E) thioridazine on mexiletine *p*-hydroxylase activity in human liver microsomes are shown. Each datum point is the average of duplicate determinations. Lines were drawn by linear regression analysis. Paroxetine and thioridazine showed mixed-type (competitive and non-competitive) inhibition and the others showed competitive inhibition. K_{is} is the inhibition constant on the slope (competitive); K_{ii} is the inhibition constant on the intercept (non-competitive).

Table I. Predicted change of *in vivo* clearance of mexiletine by psychotropic drugs.

Psychotropic drugs	I_{max} (μM)	Protein binding (%)	I_u (nM)	$I_{u,liver}$ (μM)	K_i (μM)	$1+I_{u,liver}/K_i$
Paroxetine	1.5	95	75	2.3	1.7[a]	2.4
Fluoxetine	1.5	94	90	2.7	0.6	5.5
Sertraline	0.6	98	12	0.4	7.6	1.1
Desipramine	1.1	83	187	5.6	3.2	2.8
Thioridazine	1.6	98	32	0.6	0.5[a]	2.2

[a]In the case of mixed-type inhibition, the lower K_m was used in the calculation.

mixed-type inhibition with $K_{is} = 1.7 \pm 0.7$ μM and $K_{ii} = 3.6 \pm 0.9$ μM. Fluoxetine, sertraline and desipramine exhibited competitive inhibition with $K_{is} = 0.6 \pm 0.1$, 7.6 ± 0.8 and 3.2 ± 0.5 μM, respectively. Thioridazine also exhibited mixed-type inhibition with $K_{is} = 0.5 \pm 0.2$ μM and $K_{ii} = 3.6 \pm 1.6$ μM.

Predicted change of clearance of mexiletine by psychotropic drugs from in vitro *data*

To predict the possibility of drug interaction via a metabolic process between mexiletine and the psychotropic drugs, $1 + (I/K_i)$ values were calculated (Table I). The maximum plasma concentrations of paroxetine (Kaye et al. 1989), fluoxetine (Altamura et al. 1994), sertraline (DeVane et al. 2002), desipramine (Sallee and Pollock 1990) and thioridazine (Vanderheeren and Muusze 1977; Chakraborty et al. 1989) have been reported to be 1.5, 1.5, 0.6, 1.1 and 1.6 μM, respectively. The protein binding of each psychotropic drug in plasma has been reported to be 95% for paroxetine (Kaye et al. 1989), 94% for fluoxetine (Altamura et al. 1994), 98% for sertraline (DeVane et al. 2002), 83% for desipramine (Sallee and Pollock 1990) and 98% for thioridazine (Nyberg et al. 1978). In the liver, the concentrations of paroxetine, fluoxetine (Vermeulen 1998), desipramine (Apple and Bandt 1988) and sertraline (Levine et al. 1994) have been reported to be 30-fold higher that those in plasma. Thioridazine accumulation in the liver is 20-fold higher than the plasma concentration (Dinovo et al. 1978). Accordingly, the maximum unbound liver concentrations were estimated to be 2.3 μM for paroxetine, 2.7 μM for fluoxetine, 0.4 μM for sertraline, 5.6 μM for desipramine and 0.6 μM for thioridazine. Finally, the $1 + (I/K_i)$ values calculated for paroxetine, fluoxetine, sertraline, desipramine and thioridazine were 2.4, 5.5, 1.1, 2.8 and 2.2, respectively.

Mechanism-based inactivation of human CYP enzymes

Since paroxetine has a methylenedioxy moiety in the structure, we investigated the possibility that it functions as a mechanism-based inactivator. As shown in Figure 4, paroxetine inhibited mexiletine *p*-hydroxylase activities in human liver microsomes with the NADPH-generating system in a time- and concentration-dependent manner. $K_{inact} = 0.15\ min^{-1}$ and $K_i = 0.72$ μM (Figure 4). Thioridazine did not exhibit mechanism-based inactivation (data not shown). Fluoxetine, desipramine and sertraline were not investigated since these compounds have no structure that would suggest mechanism-based inactivation.

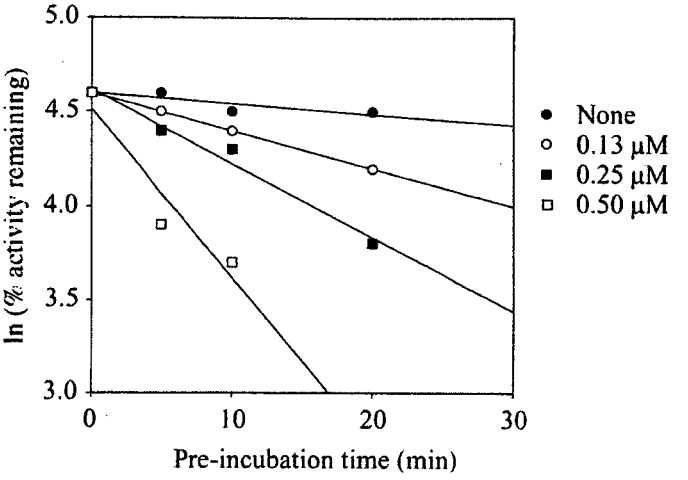

Figure 4. Mechanism-based inactivation of mexiletine *p*-hydroxylase activity in human liver microsomes by paroxetine. Pooled human liver microsomes were pre-incubated with various concentrations of paroxetine for 5, 10 and 20 min at 37°C in the presence of an NADPH-generating system. After pre-incubation, mexiletine was added to the reaction mixture and the *p*-hydroxymexiletine formed was determined. Lines were determined by linear regression of time versus the logarithm of the reaction velocity ratio. The concentration of mexiletine was 20 μM and the control activity was 3.4 pmol min^{-1} mg^{-1} protein. Data points represent the average of duplicate determinations.

Discussion

Mexiletine, an anti-arrhythmic drug, is sometimes used with psychotropic drugs in clinical practice. It has been reported that approximately 5% of the absorbed dose is excreted unchanged in human urine (Labbé and Turgeon 1999). Mexiletine is extensively metabolized, with metabolic ratios calculated as AUC of metabolite/AUC of mexiletine for *p*-hydroxymexiletine and 2-hydroxymexiletine ranging from 0.2 to 0.5 in humans (Paczkowski et al. 1990; Otani et al. 2003). It is well known that inhibition of drug metabolism of certain drugs by co-administered drugs might cause adverse reactions (Guengerich 1997; Lin and Lu 1998). Since the kinetics and the enzymes responsible for *p*-hydroxylation and 2-hydroxylation of mexiletine are almost the same (Nakajima et al. 1998), potent inhibition of mexiletine *p*-hydroxylation would imply substantial changes of *in vivo* mexiletine pharmacokinetics. In the present study, to predict the *in vivo* drug interactions between mexiletine and psychotropic drugs, the inhibitory effects of psychotropic drugs on mexiletine metabolism in human liver microsomes were investigated.

Phenytoin (metabolized mainly by CYP2C9 and to a minor extent by CYP2C19) (Bajpai et al. 1996) and carbamazepine (metabolized by CYP3A4) (Kerr et al. 1994) are anticonvulsant drugs. They are used as palliatives for lancinating pain such as trigeminal neuralgia and intractable neuropathic pain, and are sometimes used together with mexiletine. Selective serotonin re-uptake inhibitors such as fluvoxamine (metabolized by CYP2D6 and an inhibitor of CYP1A2 and CYP2C19) (Brosen et al. 1993; Harten 1995), paroxetine (metabolized by CYP2D6) (Bloomer et al. 1992), fluoxetine (metabolized mainly by CYP2D6 and to a minor extent by CYP2C9 and CYP3A4) (Fjordside et al. 1999; Margolis et al. 2000), citalopram (metabolized mainly by CYP3A4 and to a minor extent by CYP2C19)

(Kobayashi et al. 1997) and sertraline (metabolized by multiple isoforms of CYP2D6, CYP2C9, CYP2B6, CYP2C19 and CYP3A4) (Kobayashi et al. 1999; DeVane et al. 2002) are the most often prescribed antidepressants in many countries. Imipramine (metabolized by CYP2D6) (Skjelbo and Brosen 1992) and desipramine (metabolized by CYP2D6) (Von Moltke et al. 1995) are tricyclic antidepressants. Haloperidol (metabolized by CYP3A4) (Fang et al. 1997; Pan et al. 1997), a dopamine D2 receptor antagonist, is prescribed worldwide as a high-potency antipsychotic drug for the treatment of acute and chronic schizophrenia and other psychiatric disorders. Thioridazine (metabolized mainly by CYP2D6 and to minor extent by CYP2C19 and CYP1A2) (Vanderheeren and Muusze 1977; Eap et al. 1996; Carrillo et al. 1999) is piperidene-type phenothiazine that is widely used for the treatment of acute schizophrenia and related disorders. Olanzapine (metabolized mainly by UDP-glucuronosyltransferase and CYP1A2, and to a minor extent by CYP2D6) (Ring et al. 1996; Callaghan et al. 1999) is a new antipsychotic drug with a thiobenzodiazepinyl structure that is effective in the treatment of both positive and negative symptoms of schizophrenia. Quazepam and etizolam are benzodiazepine agonists that are frequently prescribed as anxiolytic and hypnoticum drugs. It has been reported that the plasma concentrations of these drugs are increased with co-administration of itraconazole, a potent CYP3A4 inhibitor (Kato et al. 2003; Araki et al. 2004).

In the present study, it was found that paroxetine ($K_i = 1.7\,\mu M$), fluoxetine ($0.6\,\mu M$), sertraline ($7.6\,\mu M$), desipramine ($3.2\,\mu M$) and thioridazine ($0.5\,\mu M$) extensively inhibited mexiletine metabolism in human liver microsomes. Mexiletine is mainly metabolized by CYP2D6 in human liver microsomes (Nakajima et al. 1998). Thus, it is reasonable to propose that psychotropic drugs that have the potential to inhibit CYP2D6 would affect mexiletine metabolism. According to the prediction of the change in the clearance of mexiletine *in vivo* from the *in vitro* data using the equation $1 + (I/K_i)$, it was found that the inhibitory effects of sertraline on mexiletine metabolism would be clinically insignificant. In contrast, it appeared that fluoxetine, desipramine, paroxetine and thioridazine could significantly inhibit mexiletine metabolism, possibly causing adverse effects such as tremors, diplopia, nausea and vomiting. In particular, the pharmacokinetic drug interaction between fluoxetine and mexiletine could result in severe adverse reactions. In the present study, bindings of the psychotropic drugs in the microsomal incubation were not considered when the K_i values were calculated. Therefore, in the case that the binding in the microsomal incubation is high, one should mind a possibility of underestimating the drug interactions.

On the other hand, psychotropic drugs may cause serious cardiovascular adverse effects such as prolonged QT interval. The risk of such adverse effects is high in individuals with a history of arrhythmias and may be potentiated by pharmacokinetic interactions with co-administered drugs (Brown et al. 2004). Mexiletine may cause ventricular tachycardia as an adverse reaction. Thus, drug interactions between mexiletine and psychotropic drugs such as paroxetine, fluoxetine, desipramine and thioridazine might be more complicated.

The mechanism-based inactivation of CYP in which a metabolite covalently binds to the enzyme to form a complex leads to irreversible inhibition (Silverman 1998). Compounds containing a methylenedioxy moiety, tertiary amine, furan ring or acetylene possibly become mechanism-based inactivators of CYP. Paroxetine has a methylenedioxy moiety in its structure. The methylenedioxy group results in the generation of carbene intermediates, which form a strong covalent complex with the iron centre of haem in CYP (Ortiz de Montellano and Correia 1995). In the present study, paroxetine inactivated the mexiletine *p*-hydroxylase activity in human liver microsomes with a $K_i = 0.72\,\mu M$ and

$k_{inact} = 0.15\,min^{-1}$. The inactivation potency was stronger than its effects on dextromethorphan demethylase in human liver microsomes ($K_i = 4.85\,\mu M$, $k_{inact} = 0.17\,min^{-1}$) that have been reported by Bertelsen et al. (2003). Once an enzyme is inactivated by a mechanism-based inactivator, the recovery of the metabolic activity depends on the synthesis of the enzyme. Thus, the turnover rate of the enzyme is one of the most important parameters in the prediction of interactions involving mechanism-based inactivation. There have been a few reports on successful predictions of *in vivo* interaction based on mechanism-based inactivation from *in vitro* data (Kanamitsu et al. 2000; Mayhew et al. 2000; Ito et al. 2003). Unfortunately, since the information on the turnover rate of most human enzymes is limited, the prediction of *in vivo* interaction by mechanism-based inactivation is difficult. Nevertheless, our data suggested that paroxetine could exhibit extensive inhibition of mexiletine metabolism as both a competitive inhibitor and mechanism-based inactivator, leading to prolonged and severe adverse effects.

In conclusion, among the 14 psychotropic drugs examined, paroxetine, fluoxetine, desipramine and thioridazine were predicted to cause drug interactions with mexiletine, which may result in adverse effects in clinical practice for patients taking mexiletine. It is important to select psychotropic drugs carefully to avoid possible drug interactions.

Acknowledgement

The authors acknowledge Mr Brent Bell for reviewing the manuscript.

References

Akechi T, Okamura H, Nishiwaki Y, Uchitomi Y. 2001. Psychiatric disorders and associated and predictive factors in patients with unresectable non small cell lung carcinoma: A longitudinal study. Cancer 92:2609–2622.

Altamura AC, Moro AR, Percudani M. 1994. Clinical pharmacokinetics of fluoxetine. Clinical Pharmacokinetics 26:201–214.

Apple FS, Bandt CM. 1988. Liver and blood postmortem tricyclic antidepressant concentrations. American Journal of Clinical Pathology 89:794–796.

Araki K, Yasui N, Fukasawa T, Aoshima T, Suzuki A, Inoue Y, Tateishi T, Otani K. 2004. Inhibition of the metabolism of etizolam by itraconazole in humans: Evidence for the involvement of CYP3A4 in etizolam metabolism. European Journal of Clinical Pharmacology 60:427–430.

Bajpai M, Roskos LK, Shen DD, Levy RH. 1996. Roles of cytochrome P4502C9 and cytochrome P4502C19 in the stereoselective metabolism of phenytoin to its major metabolite. Drug Metabolism and Disposition 24:1401–1403.

Bertelsen KM, Venkatakrishnan K, Von Moltke LL, Obach RS, Greenblatt DJ. 2003. Apparent mechanism-based inhibition of human CYP2D6 in vitro by paroxetine: Comparison with fluoxetine and quinidine. Drug Metabolism and Disposition 31:289–293.

Bloomer JC, Woods FR, Haddock RE, Lennard MS, Tucker GT. 1992. The role of cytochrome P4502D6 in the metabolism of paroxetine by human liver microsomes. British Journal of Clinical Pharmacology 33:521–523.

Brosen K, Hansen JG, Nielsen KK, Sindrup SH, Gram LF. 1993. Inhibition by paroxetine of desipramine metabolism in extensive but not in poor metabolizers of sparteine. European Journal of Clinical Pharmacology 44:349–355.

Brown CS, Farmer RG, Soberman JE, Eichner SF. 2004. Pharmacokinetic factors in the adverse cardiovascular effects of antipsychotic drugs. Clinical Pharmacokinetics 43:33–56.

Callaghan JT, Bergstrom RF, Ptak LR, Beasley CM. 1999. Olanzapine. Pharmacokinetic and pharmacodynamic profile. Clinical Pharmacokinetics 37:177–193.

Campbell NP, Kelly JG, Adgey AA, Shanks RG. 1978. The clinical pharmacology of mexiletine. British Journal of Clinical Pharmacology 6:103–108.

Carrillo JA, Ramos SI, Herraiz AG, Llerena A, Agundez JA, Berecz R, Duran M, Benitez J. 1999. Pharmacokinetic interaction of fluvoxamine and thioridazine in schizophrenic patients. Journal of Clinical Psychopharmacology 19:494–499.

Chakraborty BS, Midha KK, McKay G, Hawes EM, Hubbard JW, Korchinski ED, Choc MG, Robinson WT. 1989. Single dose kinetics of thioridazine and its two psychoactive metabolites in healthy humans: A dose proportionality study. Journal of Pharmaceutical Sciences 78:796–801.

Cooper SF, Dugal R, Elie R, Albert JM. 1979. Metabolic interaction between amitriptyline and perphenazine in psychiatric patients. Progress in Neuropsychopharmacology 3:369–376.

DeVane CL, Liston HL, Markowitz JS. 2002. Clinical pharmacokinetics of sertraline. Clinical Pharmacokinetics 41:1247–1266.

Dinovo EC, Bost RO, Sunshine I, Gottschalk LA. 1978. Distribution of thioridazine and its metabolites in human tissues and fluids obtained postmortem. Clinical Chemistry 24:1828–1830.

Eap CB, Guentert TW, Schaublin-Loidl M, Stabl M, Koeb L, Powell K, Baumann P. 1996. Plasma levels of the enantiomers of thioridazine, thioridazine 2-sulfoxide, thioridazine 2-sulfone, and thioridazine 5-sulfoxide in poor and extensive metabolizers of dextromethorphan and mephenytoin. Clinical Pharmacology and Therapeutics 59:322–331.

Fang J, Baker GB, Silverstone PH, Coutts RT. 1997. Involvement of CYP3A4 and CYP2D6 in the metabolism of haloperidol. Cellular and Molecular Neurobiology 17:227–233.

Fjordside L, Jeppesen U, Eap CB, Powell K, Baumann P, Brosen K. 1999. The stereoselective metabolism of fluoxetine in poor and extensive metabolizers of sparteine. Pharmacogenetics 9:55–60.

Goldney RD, Phillips PJ, Fisher LJ, Wilson DH. 2004. Diabetes, depression, and quality of life: A population study. Diabetes Care 27:1066–1070.

Gram LF, Overo K, Kirk L. 1974. Influence of neuroleptics and benzodiazepines on metabolism of tricyclic antidepressants in man. American Journal of Psychiatry 131:863–866.

Guengerich FP. 1997. Role of cytochrome P450 enzymes in drug–drug interactions. Advance in Pharmacology 43:7–35.

Harten J. 1995. Overview of the pharmacokinetics of fluvoxamine. Clinical Pharmacokinetics 29:1–9.

Ito K, Ogihara K, Kanamitsu S, Itoh T. 2003. Prediction of the in vivo interaction between midazolam and macrolides based on in vitro studies using human liver microsomes. Drug Metabolism and Disposition 31:945–954.

Kanamitsu S, Ito K, Okuda H, Ogura K, Watabe T, Muro K, Sugiyama Y. 2000. Prediction of in vivo drug–drug interactions based on mechanism-based inhibition from in vitro data: Inhibition of 5-fluorouracil metabolism by (E)-5-(2-bromovinyl) uracil. Drug Metabolism and Disposition 28:467–474.

Kato K, Yasui N, Fukasawa T, Aoshima T, Suzuki A, Kanno M, Otani K. 2003. Effects of itraconazole on the plasma kinetics of quazepam and its two active metabolites after a single oral dose of the drug. Therapeutic Drug Monitoring 25:473–477.

Kaye CM, Haddock RE, Langley PF, Mellows G, Tasker TC, Zussman BD, Greb WH. 1989. A review of themetabolism and pharmacokinetics of paroxetine in man. Acta Psychiatrica Scandinavica Supplementum 350:60–75.

Kerr BM, Thummel KE, Wurden CJ, Klein SM, Kroetz DL, Gonzalez FJ, Levy RH. 1994. Human liver carbamazepine metabolism. Role of CYP3A4 and CYP2C8 in 10,11-epoxide formation. Biochemical Pharmacology 47:1969–1979.

Kobayashi K, Chiba K, Yagi T, Shimada N, Taniguchi T, Horie T, Tani M, Yamamoto T, Ishizaki T, Kuroiwa Y. 1997. Identification of cytochrome P450 isoforms involved in citalopram N-demethylation by human liver microsomes. Journal of Pharmacology and Experimental Therapeutics 280:927–233.

Kobayashi K, Ishizuka T, Shimada N, Yoshimura Y, Kamijima K, Chiba K. 1999. Sertraline N-demethylation is catalyzed by multiple isoforms of human cytochrome P-450 in vitro. Drug Metabolism and Disposition 27:763–766.

Kugaya A, Akechi T, Okuyama T, Nakano T, Mikami I, Okamura H, Uchitomi Y. 2000. Prevalence, predictive factors, and screening for psychologic distress in patients with newly diagnosed head and neck cancer. Cancer 88:2817–2823.

Kurtz DL, Bergstrom RF, Goldberg MJ, Cerimele BJ. 1997. The effect of sertraline on the pharmacokinetics of desipramine and imipramine. Clinical Pharmacology and Therapeutics 62:145–156.

Labbé L, Turgeon J. 1999. Clinical pharmacokinetics of mexiletine. Clinical Pharmacokinetics 37:361–384.

Lane RM. 1996. Pharmacokinetic drug interaction potential of selective serotonin reuptake inhibitors. International Clinical Psychopharmacology 11:31–61.

Levine B, Jenkins AJ, Smialek JE. 1994. Distribution of sertraline in postmortem cases. Journal of Analytical Toxicology 18:272–274.

Lin JH, Lu AY. 1998. Inhibition and induction of cytochrome P450 and the clinical implications. Clinical Pharmacokinetics 35:361–390.

Margolis JM, O'Donnell JP, Mankowski DC, Ekins S, Obach RS. 2000. (R)-, (S)-, and racemic fluoxetine N-demethylation by human cytochrome P450 enzymes. Drug Metabolism and Disposition 28:1187–1191.

Mayhew BS, Jones DR, Hall SD. 2000. An in vitro model for predicting in vivo inhibition of cytochrome P450 3A4 by metabolic intermediate complex formation. Drug Metabolism and Disposition 28:1031–1037.

Nakajima M, Kobayashi K, Shimada N, Tokudome S, Yamamoto T, Kuroiwa Y. 1998. Involvement of CYP1A2 in mexiletine metabolism. British Journal of Clinical Pharmacology 46:55–62.

Nakajima M, Suzuki M, Yamaji R, Takashina H, Shimada N, Yamazaki H, Yokoi T. 1999. Isoform selective inhibition and inactivation of human cytochrome P450s by methylenedioxyphenyl compounds. Xenobiotica 29:1191–1202.

Nyberg G, Axelsson R, Martensson E. 1978. Binding of thioridazine and thioridazine metabolites to serum proteins in psychiatric patients. European Journal of Clinical Pharmacology 14:341–350.

Okamura H, Watanabe T, Narabayashi M, Katsumata N, Ando M, Adachi I, Akechi T, Uchitomi Y. 2000. Psychological distress following first recurrence of disease in patients with breast cancer: Prevalence and risk factors. Breast Cancer Research and Treatment 61:131–137.

Ortiz de Montellano PR, Correia MA. 1995. Inhibition of cytochrome P450 enzymes. In: PR Ortiz de Montellano, editor. Cytochrome P450 structure, mechanism and biochemistry. New York: Plenum. pp 305–366.

Otani M, Fukuda T, Naohara M, Maune H, Senda C, Yamamoto I, Azuma J. 2003. Impact of CYP2D6*10 on mexiletine pharmacokinetics in healthy adult volunteers. European Journal of Clinical Pharmacology 59:395–399.

Paczkowski D, Sadowski Z, Filipek M, Kolinski P. 1990. Pharmacokinetics of mexiletine and its metabolites, hydroxymethylmexiletine and p-hydroxymexiletine, after single oral administration in healthy subjects. Polish Journal of Pharmacology and Pharmacy 42:365–375.

Pan LP, Wijnant P, Vriendt C, Rosseel MT, Belpaire FM. 1997. Characterization of the cytochrome P450 isoenzymes involved in the in vitro N-dealkylation of haloperidol. British Journal of Clinical Pharmacology 44:557–564.

Preskorn SH. 1998. Debate resolved: There are differential effects of serotonin selective reuptake inhibitors on cytochrome P450 enzymes. Journal of Psychopharmacology 12:S89–97.

Ring BJ, Catlow J, Lindsay TJ, Gillespie T, Roskos LK, Cerimele BJ, Swanson SP, Hamman MA, Wrighton SA. 1996. Identification of the human cytochromes P450 responsible for the in vitro formation of the major oxidative metabolites of the antipsychotic agent olanzapine. Journal of Pharmacology and Experimental Therapeutics 276:658–666.

Sallee FR, Pollock BG. 1990. Clinical pharmacokinetics of imipramine and desipramine. Clinical Pharmacokinetics 18:346–364.

Segel IH, editor. 1993. Rapid equilibrium partial and mixed type inhibition. In: Enzyme kinetics. New York: Wiley-Interscience. pp 161–226.

Silverman RB, editor. 1988. Mechanism-based enzyme inactivation. In: Chemistry and enzymology. Vol. 1. Boca Raton, FL: CRC Press. pp 3–30.

Skjelbo E, Brosen K. 1992. Inhibitors of imipramine metabolism by human liver microsomes. British Journal of Clinical Pharmacology 34:256–261.

Uchitomi Y, Mikami I, Nagai K, Nishiwaki, Y, Akechi T, Okamura H. 2003. Depression and psychological distress in patients during the year after curative resection of non-small-cell lung cancer. Journal of Clinical Oncology 21:69–77.

Vanderheeren FA, Muusze RG. 1977. Plasma levels and half lives of thioridazine and some of its metabolites I. High doses in young acute schizophrenics. European Journal of Clinical Pharmacology 11:135–140.

Vermeulen T. 1998. Distribution of paroxetine in three postmortem cases. Journal of Analytical Toxicology 22:541–544.

Von Moltke LL, Greenblatt DJ, Court MH, Duan SX, Harmatz JS, Shader RI. 1995. Inhibition of alprazolam and desipramine hydroxylation in vitro by paroxetine and fluvoxamine: Comparison with other selective serotonin reuptake inhibitor antidepressants. Journal of Clinical Psychopharmacology 15:125–131.

TOXICOLOGICAL SCIENCES 87(1), 296–305 (2005)
doi:10.1093/toxsci/kfi235
Advance Access publication June 23, 2005

Relationship between Hepatic Gene Expression Profiles and Hepatotoxicity in Five Typical Hepatotoxicant-Administered Rats

Keiichi Minami,* Toshiro Saito,† Masatoshi Narahara,† Hiroyuki Tomita,† Hirokazu Kato,† Hisashi Sugiyama,† Miki Katoh,* Miki Nakajima,* and Tsuyoshi Yokoi*,[1]

*Drug Metabolism and Toxicology, Division of Pharmaceutical Sciences, Kanazawa University, Kanazawa, Japan, and †Life science group, Hitachi Ltd., Saitama, Japan

Received May 27, 2005; accepted June 2, 2005

In the field of gene expression analysis, DNA microarray technology has a major impact on many different areas including toxicogenomics, such as in predicting the adverse effects of new drug candidates and improving the process of risk assessment and safety evaluation. In this study, we investigated whether there is relationship between the hepatotoxic phenotypes and gene expression profiles of hepatotoxic chemicals measured by DNA microarray analyses. Sprague-Dawley rats (6 weeks old) were administered five hepatotoxicants: acetaminophen (APAP), bromobenzene, carbon tetrachloride, dimethylnitrosamine, and thioacetamide. Serum biochemical markers for liver toxicity were measured to estimate the maximal toxic time of each chemical. Hepatic mRNA was isolated, and the gene expression profiles were analyzed by DNA microarray containing 1,097 drug response genes, such as cytochrome P450s, other phase I and phase II enzymes, nuclear receptors, signal transducers, and transporters. All the chemicals tested generated specific gene expression patterns. APAP was sorted to a different cluster from the other four chemicals. From the gene expression profiles and maximal toxic time estimated by serum biochemical markers, we identified 10 up-regulated genes and 10 down-regulated genes as potential markers of hepatotoxicity. By Quality-Threshold (QT) clustering analysis, we identified major up- and down-regulated expression patterns in each group. Interestingly, the average gene expression patterns from the QT clustering were correlated with the mean value profiles from the biochemical markers. Furthermore, this correlation was observed at any extent of hepatotoxicity. In this study, we identified 17 potential toxicity markers, and those expression profiles could estimate the maximal toxic time independently of the hepatotoxicity levels. This expression profile analysis could be one of the useful tools for evaluating a potential hepatotoxicant in the drug development process.

Key Words: gene expression profiles; hepatotoxicity; DNA microarray.

The aim of toxicological studies is to detect adverse effects of a chemical on an organism based on observed toxicity markers (i.e., serum biochemical markers and chemical-specific gene expression) or phenotypic outcomes. In the past several years, novel systems, especially microarray technology, have been developed, allowing the simultaneous measurement of gene expression at the RNA level. Microarray technology can be used to elucidate the mechanisms of chemical-induced toxicity and have the possibility of being used as a tool for predicting the adverse effects of new drug candidates and improving the process of risk assessment and safety evaluation.

The liver is one of the first organs to be exposed to peroral-administered chemicals via the portal vein. Chemical concentrations in the liver are often much higher than the peak plasma concentration. The liver is also the major site for xenobiotic metabolism, and various chemicals can lead to the formation of active metabolites with toxic effects. The high concentration exposure and metabolic activity make the liver one of the primary targets for various types of chemical-induced toxicity.

The five typical hepatotoxicants chosen in this study were acetaminophen (APAP, *p*-acetamidophenol), bromobenzene (BB), carbon tetrachloride (CT), dimethylnitrosamine (DMN), and thioacetamide (TA). APAP is known as a mild analgesic drug, but it is a potent hepatotoxicant at high doses and in persons with enhanced susceptibility. APAP is largely (apparently more than 80%) converted to conjugates of glucuronate and sulfate. A minor amount, less than 5%, is metabolized to an active metabolite, mainly *N*-acetyl-*p*-benzoquinone imine (NAPQI) by cytochrome P450 (CYP) 2E1, which binds promptly to glutathione (GSH). Other metabolites (5 to 15%) appear to have no toxicity (Zimmerman, 1999). When an active metabolite exceeds the GSH content, excess metabolite binds to tissue molecules and manifests toxicity such as necrosis. BB, a traditional hepatotoxicant, is subjected to cytochrome P450-mediated epoxidation, and a major metabolite is 3,4-epoxide. Detoxication of the active metabolite is by GSH conjugation. At high BB doses, due to the conjugation to the epoxides, liver GSH shortage and secondary reactions such as lipid peroxidation, intracellular calcium alteration, and mitochondrial dysfunction

[1] To whom correspondence should be addressed at Drug Metabolism and Toxicology, Division of Pharmaceutical Sciences, Kanazawa University, Kakuma-machi, Kanazawa 920-1192, Japan. Fax: +81-76-234-4407. E-mail: tyokoi@kenroku.kanazawa-u.ac.jp.

finally lead to cell death (Heijne *et al.*, 2003, Zimmerman, 1999). CT is a potent hepatotoxicant, and a single dose leads promptly to severe necrosis and steatosis. CT liver necrosis is caused by trichloromethyl free radicals from a CYP2E1-mediated pathway. The covalent binding of trichloromethyl to cell protein is considered the initial step of sequential events leading to membrane lipid peroxidation and, finally, to cell necrosis (Jeong, 1999; Zimmerman, 1999). DMN is the most potent toxicant of all dialkylnitrosamines and leads to hemorrhagic necrosis and steatosis. The DMN toxicity process is as follows: first, demethylation of CYP2E1 to monomethylnitrosamine; second, spontaneous change of diasomethane; finally, methylation of cell components (Zimmerman, 1999). Thioacetamide (TA) is a potent hepatotoxicant that requires metabolic activation by mixed-function oxidases. Generally, CYP2B, CYP2E1, and FMOs metabolize TA to its toxic metabolites (Hunter *et al.*, 1977; Wang *et al.*, 2000), and these intermediate metabolites might bind to cellular proteins by the formation of acetylimidolysine derivatives (Dyroff and Neal, 1981). TA is apparently converted to thioacetamide-*S*-oxide and is presumably converted to an active toxic metabolite that binds covalently to tissue molecules, provoking necrosis (Zimmerman, 1999).

The aims of this study were to find available toxicity marker genes, to investigate the correlation between biochemical markers and gene expression profiles, and to create a new evaluation method using DNA microarray. In this study, we attempted to apply our microarray of drug-response gene expressions for the evaluation of chemical-induced hepatotoxicity in rats.

MATERIALS AND METHODS

Animals and chemicals. Male Sprague-Dawley rats (5-week old, 130–150 g) were obtained from SLC Japan (Hamamatsu, Japan). Animals were housed in a controlled environment (temperature 25 ± 1°C, humidity 50 ± 10%, and 12-h light/12-h dark cycle) in the institutional animal facility with access to food and water *ad libitum*. Animals were acclimatized for a week before use in experiments. Animal maintenance and treatment were conducted in accordance with the National Institutes of Health Guide for Animal Welfare of Japan, as approved by Institutional Animal Care and Use Committee of Kanazawa University, Japan. APAP, BB, CT, DMN, and TA were obtained Wako Pure Chemical Industries (Osaka, Japan). ISOGEN, RNA extraction reagent was from Nippon Gene (Tokyo, Japan). *N*-hydroxysuccinimide (NHS)-ester Cy3 or Cy5 was from GE Healthcare Amersham Biosciences (Buckinghamshire, UK). ReverTra Ace (Moloney Murine Leukemia Virus Reverse Transcriptase RnaseH Minus) was from Toyobo (Tokyo, Japan). Random hexamer and SYBR® Premix Ex Taq™ (Perfect Real Time) were from Takara (Osaka, Japan). All primers were commercially synthesized at Hokkaido System Sciences (Sapporo, Japan). Other chemicals were of the highest grade commercially available.

Administration of chemicals and assessment of liver injury. Eighty-eight rats were assigned to 22 groups (four rats/group). The dosing solutions were prepared as follows with each vehicle. APAP: 500 mg/kg in corn oil; BB: 2.5 mmol/kg in corn oil; CT: 1 ml/kg in corn oil; DMN: 20 mg/kg in saline; TA: 400 mg/kg in saline; control: vehicle for saline or corn oil group. The chemicals were intraperitoneally injected in a single bolus at a volume of 2 ml/kg. At the indicated time (6, 12, 24, 48 h after administration), the rats were sacrificed, and the liver and serum samples were collected. Four typical biochemical markers for hepatotoxicity (aspartate aminotransferase, AST; alanine aminotransferase, ALT; lactate dehydrogenase, LDH; alkaline phosphatase, ALP) were measured by SRL, Inc. (Tokyo, Japan).

RNA isolation. Total hepatic RNA was isolated using ISOGEN. Approximately 100 mg of whole liver were lysed with 1.0 ml of the lysis solution. Chloroform (200 μl) was added and vortexed vigorously for 15 s. The mixture was centrifuged at 15,000 × *g* for 15 min at 4°C. The aqueous phase was transferred carefully to a new tube, and the RNA was precipitated with 0.5 ml of isopropyl alcohol for 10 min at room temperature. The mixture was centrifuged at 15,000 × *g* for 10 min. After washing with 75% ethanol, the pellet was dissolved in diethylpyrocarbonate-treated water. Equal amounts of total mRNA from each hepatotoxicant-administered sample were pooled and used for the microarray analysis and real-time reverse transcriptase (RT)-PCR.

In vitro amplification and DNA microarray. cDNA targets were prepared from pooled total RNA by *in vitro* transcription reaction as described previously (Luo *et al.*, 1999). Amplified RNA (6 μg) was reverse transcribed by random hexamer and aminoallyl-dUTP. The synthesized cDNA was labeled with NHS-ester Cy3 or Cy5 (Hughes *et al.*, 2001). The labeled cDNA was applied to the cDNA microarray (Rat Drug Response Chip containing 1,097 genes, Hitachi, Tokyo, Japan). In order to confirm the microarray data in the APAP group, a Rat cDNA Microarray kit G4105A containing 14,815 genes (Agilent Technologies, Palo Alto, CA) was used. Hybridization was performed at 62°C for 14 h. After washing, the microarray was scanned on a ScanArray 5000 (Packard BioChip Technologies, Billerica, MA), and the image was analyzed using QuantArray software (Packard BioChip Technologies). The signal intensity of each spot was calibrated by subtraction of the intensity of the control.

Real-time RT-PCR. Rat Cathepsin L (CtsL), Diazepam binding inhibitor (Dbi), Heme oxygenase 1 (Hmox1), Sulfotransferase 1a2 (Sult1a2), T-cell death associated gene (Tdag), and GAPDH were quantified by real-time RT-PCR. Primer sequences using in this study were as follows: CtsL, 5′-TCT ACT ATG AAC CCA ACT G-3′ and 5′-GAT TCA AGT ACC ATG GTC T-3′; Dbi, 5′-CCA ACT GAT GAA GAG ATG CTG T-3′ and 5′-CCC TAA CAT ATC AGA GCC ATG T-3′; Hmox1, 5′-ATA GAG CGA AAC AAG CAG A-3′ and 5′-TAG AGC TGT TTG AAC TTG G-3′; Sult1a2, 5′-TCA TTG AGT GGA CTT TGC CTT-3′ and 5′-CAC TTT TCC AGC TTT GAA CTG-3′; Tdag, 5′-CCA AGC AGG TAC AAC ATC AG-3′ and 5′-TTC TGC CTC GTA GAC TTG AC-3′. For RT process, total RNA (4 μg) and 150 ng random hexamer were mixed and incubated at 70°C for 10 min. RNA solution was added to a reaction mixture containing 100 units of ReverTra Ace, reaction buffer, and 0.5 mM dNTPs in a final volume of 40 μl. The reaction mixture was incubated at 30°C for 10 min, 42°C for 1 h, and heated at 98°C for 10 min to inactivate the enzyme. Real-time PCR was performed using the Smart Cycler® (Cepheid, Sunnyvale, CA) with Smart Cycler® software (Ver. 1.2b). PCR mixture contained 1 μl of template cDNA, SYBR® Premix Ex Taq™ solution and 10 pmol of sense and antisense primers. The PCR condition for GAPDH and Sult1a2 was as follows: after an initial denaturation at 95°C for 30 s, the amplification was performed by denaturation at 94°C for 4 s, annealing and extension at 64°C for 20 s for 45 cycles. The PCR condition for other genes was as follows: after an initial denaturation at 95°C for 20 s, the amplification was performed by denaturation at 95°C for 5 s, annealing at 55°C for 10 s, and extension at 72°C for 15 s for 45 cycles. Amplified products were monitored directly by measuring the increase of the dye intensity of the SYBR Green I (Molecular Probes, Eugene, OR) that binds to double-strand DNA amplified by PCR.

Data management. Fold-change determination, experiment normalization, and clustering analysis were performed with GeneSpring software (Agilent Technologies). Gene expression values for each chip were normalized to the intensity-dependent (LOWESS) normalization built in GeneSpring. In the Quality-Threshold (QT) clustering analyses, a standard correlation method was used in this study. Fold-change filters included the requirement that the

TABLE 1
Changes of Biochemical Markers in Five Chemical-Administered Rats

Chemical	Time(h)	AST (IU/l)	ALT (IU/l)	LDH (IU/l)	ALP (IU/l)
Control (corn oil)	48	152 ± 7	60 ± 3	2647 ± 248	1711 ± 128
Control (saline)	48	177 ± 22	55 ± 9	3528 ± 566	1499 ± 49
Acetaminophen (APAP)	6	239 ± 18[a]	72 ± 8	3590 ± 265	1184 ± 85[a]
	12	294 ± 66[a]	78 ± 13	4001 ± 480	1222 ± 53[a]
	24	187 ± 28	56 ± 7	4240 ± 1130	1478 ± 176
	48	248 ± 68	81 ± 17	3949 ± 684	1283 ± 123
Bromobenzene (BB)	6	177 ± 14	49 ± 5[a]	4088 ± 708	1625 ± 7
	12	178 ± 14	41 ± 1[b]	3891 ± 476	1239 ± 51[a]
	24	476 ± 88[a]	120 ± 23[a]	5785 ± 248[b]	1876 ± 181
	48	618 ± 206	259 ± 76[a]	4068 ± 1023	1403 ± 163
Carbon tetrachloride (CT)	6	1196 ± 155[b]	411 ± 75[b]	6284 ± 962[a]	1638 ± 207
	12	782 ± 317	303 ± 147	4079 ± 399	1123 ± 46[a]
	24	595 ± 163[a]	248 ± 94	3533 ± 579	1154 ± 112[a]
	48	2059 ± 651[a]	706 ± 156[b]	3120 ± 487	1328 ± 170
Dimethylnitrosamine (DMN)	6	217 ± 26	60 ± 8	2933 ± 558	1516 ± 144
	12	266 ± 70	84 ± 24	2278 ± 303	1486 ± 314
	24	186 ± 15	88 ± 5[a]	1038 ± 153[b]	1848 ± 187
	48	426 ± 28[b]	192 ± 24[b]	846 ± 21[b]	1182 ± 100
Thioacetamide (TA)	6	198 ± 8	52 ± 2	3586 ± 429	1344 ± 149
	12	287 ± 18[b]	75 ± 4	3180 ± 239	1817 ± 53[b]
	24	8312 ± 1735[b]	1749 ± 371[b]	53083 ± 9662[b]	1682 ± 89
	48	1933 ± 405[b]	487 ± 91[a]	3976 ± 219	2174 ± 342

Note. Data are expressed as mean ± SE ($n = 4$).
[a]Significantly different from control group ($p < 0.05$).
[b]Significantly different from control group ($p < 0.01$).

genes be present in at least 200% of the administered samples for up-regulated genes, and 50% of controls for down-regulated genes.

Statistics. The *t*-test was used to detect significant differences between the means of two groups relative to the observed variance within groups.

RESULTS

Assessment of Liver Toxicity

The serum biochemical markers in the five chemical-administered groups were measured at 6, 12, 24, and 48 h after administration (Table 1). The AST activities of the APAP-, BB-, CT-, DMN-, and TA-administered groups were significantly high at 12, 24, 6, 48, and 24 h after administration, respectively. The changes of the ALT activities showed almost the same pattern as the AST activities in all groups. The LDH activity increased significantly in the BB-, CT-, and TA-administered groups at 24, 6, and 24 h, respectively. In the DMN-administered group, the LDH activity significantly decreased at 24 and 48 h in a time-dependent manner. In the APAP-administered group, no significant change was observed. The ALP activity decreased significantly in the APAP-, BB-, and CT-administered groups at 6 and 12, 12, and 12 and 24 h, respectively. In the TA-administered group, the ALP activity significantly increased at 12 h. In the DMN-administered group, no significant change of the ALP activity was observed. Taking these results into consideration, the maximal toxic times of APAP, BB, CT, DMN, and TA were estimated as 12, 24, 6, 48, and 24 h, respectively.

Genes Significantly Changed by at Least Four Chemicals at the Toxic Time Points

Analysis of the gene expression profile showed that 52 (25 up-regulated and 27 down-regulated) of 1,097 genes were changed above 2-fold by at least four chemicals at the maximal toxic times described above (Table 2). Eleven genes were changed above 2-fold in all the chemical administered groups (3 up-regulated and 8 down-regulated, Table 2), and 40 genes in four of the five chemical administered groups (21 up-regulated and 19 down-regulated, Table 2).

The genes in Table 2 are presented by two-way hierarchical clustering (Fig. 1). In the up-regulated genes at the maximal toxic times (Fig. 1A), CT-, TA-, and BB-administered groups were sorted in a similar cluster. However, all APAP-administered groups were sorted in a different cluster from other groups. The DMN-administered groups from 12 to 48 h were sorted in a similar cluster. Among the down-regulated genes at the maximal toxic times (Fig. 1B), those of the CT- and TA-administered groups, BB- and DMN-administered groups, and APAP-administered groups were sorted in a similar cluster,

TABLE 2
Genes Changed of Their Expression in At Least Four Chemical-Administered Rats

Gene name	Genbank ID	Common name	Pass chemicals
Up regulation			
Heme oxygenase	NM_012580	Hmox1	5
Diaphorase (NADH/NADPH)	J02679	Dia4	5
T-cell death associated gene	NM_017180	Tdag	5
P-glycoprotein/multidrug resistance 1	AF257746	Pgy1	5
Janus kinase 2 (a protein tyrosine kinase)	U13396	Jak2	4
Gro	NM_030845	Gro1	4
Heat shock cognate protein 70	NM_024351	Hsc70	4
RNA polymerase I (127 kDa subunit)	NM_031773	Rpo1-2	4
Small inducible gene JE	Scya2	Scya2	4
Thioredoxin reductase 1	NM_031614	Txnrd1	4
Heat shock protein 70-1	Z75029	Hspa1a	4
Lysozyme	NM_012771	Lyz	4
mRNA for alpha-2u globulin-related protein	X13295	Lcn2	4
Aldose-reductase-like protein MVDP/AKR1-B7 mRNA, complete cds	AF182168	Rn.32702	4
Interferon inducible protein 10 (IP-10) mRNA, complete cds	U22520	Rn.10584	4
VESP11 mRNA for vascular endothelial cell specific protein 11, complete cds	AB027561	Rn.65187	4
Aldolase A, fructose-bisphosphate	NM_012495	Aldoa	4
Caspase 3, apoptosis related cysteine protease (ICE-like cysteine protease)	U49930	Casp3	4
Potassium channel, subfamily K, member 3	U02316	Kcnk3	4
Cyclin G1	X70871	Ccng1	4
DNA-damage-inducible transcript 1	NM_024127	Gadd45a	4
Glutathione synthetase gene	L38615	Gss	4
3-hydroxy-3-methylglutaryl-Coenzyme A reductase	X55286	Hmgcr	4
Activating transcription factor 3	NM_012912	Atf3	4
Cathepsin L	Y00697	Ctsl	4
Down regulation			
sulfotransferase family 1A, phenol-preferring, member 2	NM_031732	Sult1a2	5
Rattus norvegicus NADPH oxidase 4 mRNA, complete cds	AY027527	Rn.14744	5
Gastrin	NM_012849	Gas	5
Stearoyl-CoA desaturase-1 (SCD-1)	NM_139192	Scd1	5
Sulfonylurea receptor	NM_013039	Sur	5
Thyroid stimulating hormone receptor	NM_012888	Tshr	5
Thyroid hormone receptor	X12744	Thra	5
Brain digoxin carrier protein mRNA, complete cds	U88036	Rn.5641	5
Neurotrophin 5 (neurotrophin 4/5)	NM_013184	Ntf5	4
Ornithine aminotransferase	NM_022521	Oat	4
Triadin 1	AJ243304	Trdn	4
Neuropeptide Y5 receptor	U66274	Npy5r	4
Transforming growth factor beta stimulated clone 22	NM_013043	Tgfb1i4	4
Retinoblastoma 1 (including osteosarcoma)	L07126	Rb1	4
mRNA for V1a arginine vasopressin receptor	Z11690	Rn.32282	4
Cytochrome P450 2D18 mRNA, complete cds	U48220	Cyp2d18	4
L-3-hydroxyacyl-CoA dehydrogenase precursor (HAD) mRNA, complete cds	AF095449	Rn.17172	4
ATPase inhibitor (rat mitochondrial IF1 protein)	AF368860	Atpi	4
Diazepam binding inhibitor (GABA receptor modulator, acyl-Coenxyme A binding protein)	M20268	Dbi	4
Expressed in non-metastatic cells 3, protein (nucleoside diphosphate kinase)	AY017337	Nme3	4
Insulin-like growth factor-I mRNA, 3′ end	X06108	Rn.6282	4
Estrogen sulfotransferase	NM_012883	Ste	4
Galanin receptor 3	NM_019173	Galr3	4
Pim-1 oncogene	X63675	Pim1	4
Carbonic anhydrase 2	X58294	Ca2	4
CL1BA protein	U72487	CL1BA	4
Epidermal growth factor	U04842	Egf	4

Note. Gene whose expressions were altered more than 2.0-fold at the maximal toxic time by at least four of the five chemicals. APAP: 12 h; BB: 24 h; CT: 6 h; DMN: 48 h; TA: 24 h.

respectively. In both cluster analyses, 6 and 12 h of the CT-administered groups and 24 h of the TA-administered groups were sorted in a similar cluster.

Gene Expression Profiles and Maximal Toxic Time

The peak profiles of 10 up- or down-regulated genes in Table 2 were each overlapped at the maximal toxic times (Fig. 2). The expression profiles in each of the chemical-administered groups showed similar patterns at all the time points investigated in the present study.

To confirm the gene expression profiles of DNA microarray as shown in Figure 2, real-time RT-PCR was performed (Fig. 3). The expression profiles of all five genes were almost the same as those of DNA microarray. The extent of these gene expressions was higher than that of DNA microarray.

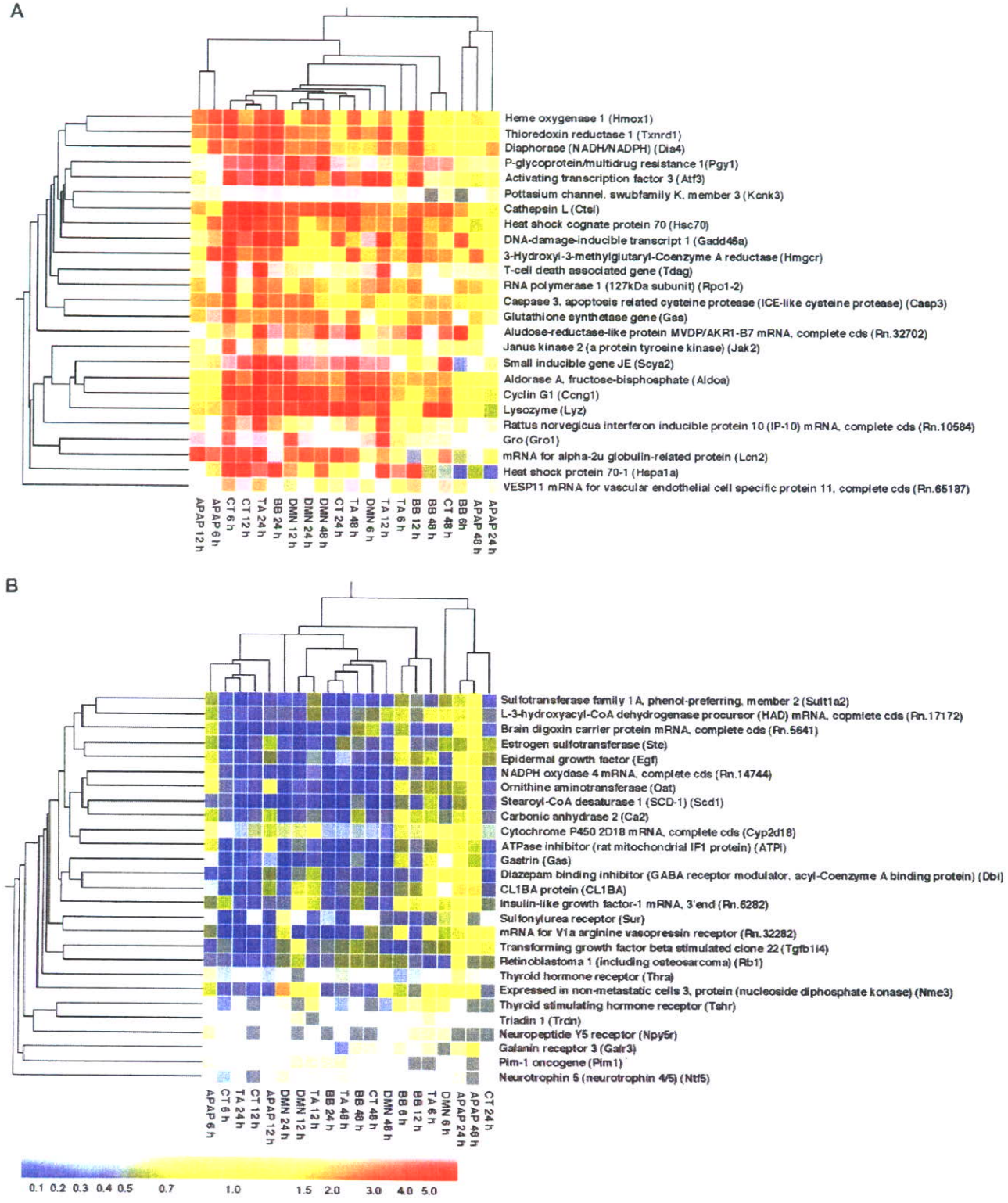

FIG. 1. Two-way hierarchical cluster images of genes whose expressions were altered more than 2-fold at the maximal toxic times by at least four chemicals. The results of hierarchical cluster analyses are shown with a dendrogram for (A) 25 up-regulated genes and (B) 27 down-regulated genes listed in Table 2. Gene expression data are expressed as fold of control values, and the range of change represented by colors at the bottom of the cluster images. The expression pattern of each gene is displayed here as a horizontal strip.

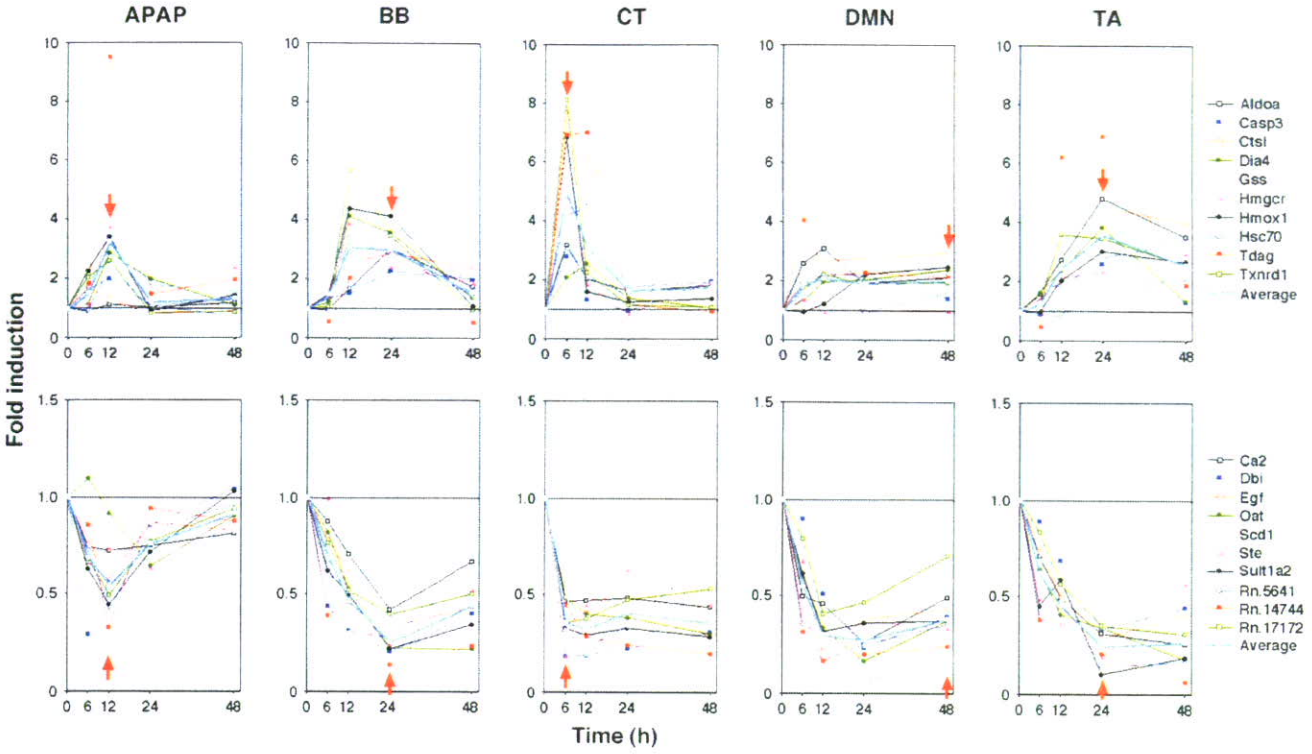

FIG. 2. Time-dependent changes of the expressions of 20 representative genes in Table 2. The peaks of the expression in up- or down-regulated genes were overlapped with the maximal toxic times examined in the present study. Red arrows indicate the maximal toxic time in each chemical-administrated group estimated from the change of biochemical markers. Official gene name is described in Table 2.

QT Clustering for Minimal Correlation

In order to estimate the majority of the gene expression profiles, QT clustering analysis was performed. In this process, we used the GeneSpring QT clustering algorism. The analysis setting for the minimal cluster size was 100 genes, and the minimal correlation coefficient was 0.5 for the Rat Drug Response Chip containing 1,097 genes. Probes with a certain expression level higher than 0.01 in all the administered samples (759 of 1,097 genes) were used. In all groups, the up-regulated and down-regulated types of clusters were identified and expressed as average values (Fig. 4A). In the up-regulated type cluster, the APAP-, BB-, CT-, DMN-, and TA-administered groups contained 109, 105, 143, 139, and 153 genes, respectively (upper part of Fig. 4A). The down-regulated type clusters of the APAP-, BB-, CT, DMN-, and TA-administered groups contained 122, 159, 180, 144, and 163 genes, respectively (lower part of Fig. 4A). As a result, all clusters except those of DMN reflected the maximal toxic time.

In order to confirm the data with the Rat Drug Response Chip, analysis with Agilent Rat cDNA microarray kit G4105A was performed only in the APAP-administered group. QT clustering was also performed, and the analysis setting for the minimal cluster size was 1,000 genes, and the minimal correlation coefficient was 0.68. Probes with a certain expression level higher than 0.01 in all administered samples (14,474 of 14,815 genes) were used. Up-regulated and down-regulated type clusters contained 1,058 and 1,106 genes, respectively, and were expressed as mean values (Fig. 4B). As expected, both clusters of APAP showed almost the same profiles as those of the Rat Drug Response Chip.

Genes Appeared in All Five of the Chemical-Administered Groups

For further analysis, the gene expression profiles identified in the gene clusters of all chemicals in Figure 4A were displayed. Three genes were contained in all the up-regulated type clusters and 17 genes in the down-regulated type clusters of all the chemical-administered groups as shown in Figure 4. The expression profiles of 17 down-regulated genes are shown in Figure 4A. The blue lines indicate the expression profiles of the genes that appeared not only in Figure 2 but also in Figure 4. The expression profiles of the genes that appeared in all chemical groups but only in Figure 4 are indicated by black lines. The three common genes in the up-regulated type cluster were not listed in Figure 2 (data not shown). In the down-regulated type cluster, eight genes of all the regulated groups were also listed in Figure 2. The 3 up-regulated and 17 down-regulated genes were analyzed in the following QT clustering.

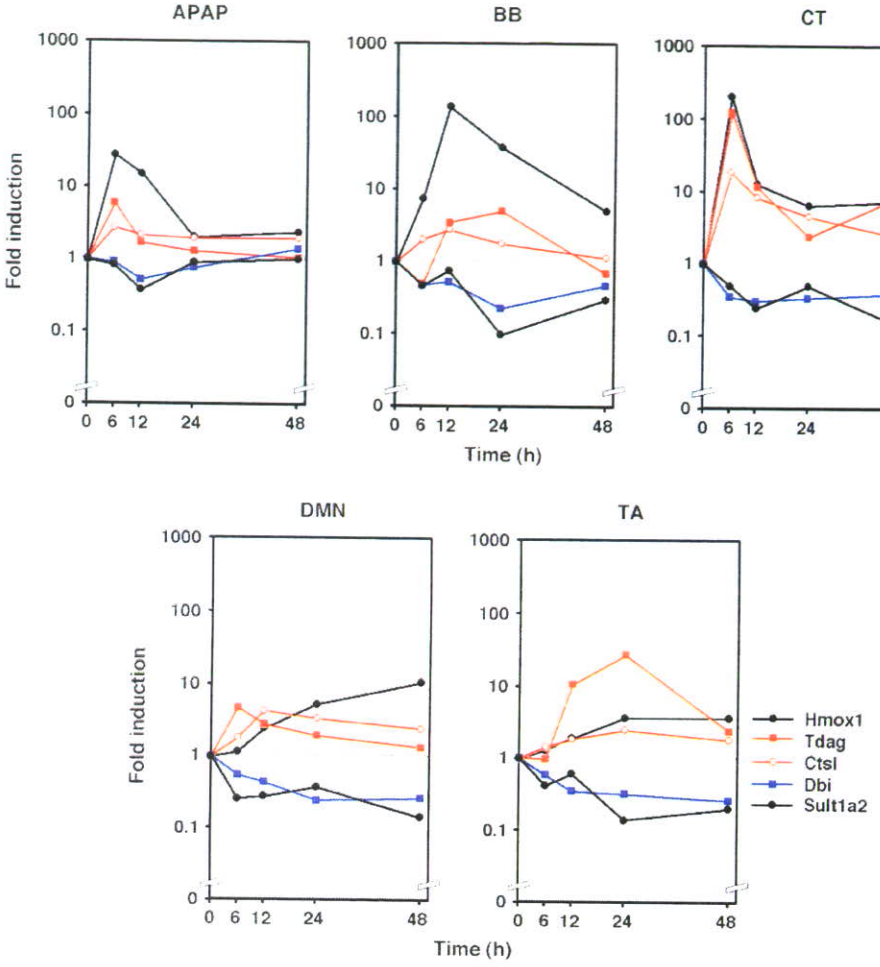

FIG. 3. Real-time RT-PCR analysis of the expression of the representative genes. Total RNA samples from four rats were pooled and used for real-time RT-PCR analysis. This figure contains the representative three up-regulated and two down-regulated genes as shown in Figure 2. Official gene name is described in Table 2.

QT Clustering for the Genes That Appeared in at Least Four of Five Chemical-Administered Groups

For further analysis, the genes that appeared in at least four of the five chemical-administered groups were analyzed. Thirty-seven genes were identified in the up-regulated type cluster and 60 genes in the down-regulated type cluster, as shown in Figure 4. In the up-regulated type cluster, 7 of 37 genes were overlapped with the genes of the up-regulated groups shown in Figure 2. In the down-regulated type cluster, all genes of the down-regulated groups in Figure 2 were overlapped. Further QT clustering was performed using the 37 up-regulated or 60 down-regulated genes identified in Figure 4A. The analysis setting for the minimal cluster size was 10 genes and the minimal correlation coefficient was 0.65. Twenty-two of 37 genes were identified as the up-regulated type cluster, and 44 of 60 genes as the down-regulated type cluster. The profiles of the 22 and 44 identified genes and the average profile are shown in Figures 5B and 5C, respectively. The expression profiles of the genes that also appeared in Figure 2 are indicated by blue lines. The expression profiles of the clustered gene that did not appear in Figure 2 are indicated by black lines. Seven of 10 genes in the up-regulated group in Figure 2 and all 10 genes in the down-regulated group in Figure 2 were overlapped as a result of the clustering (Figs. 5B and 5C). As shown in Figures 5A, 5B, and 5C, the average up-regulated or down-regulated peaks were correlated with the maximal toxic times.

DISCUSSION

Gene expression changes have been used routinely to obtain specific mechanistic information concerning the type of action of a toxicant. Toxicogenomics is an approach that applies microarray technology to toxicological evaluation paradigms.

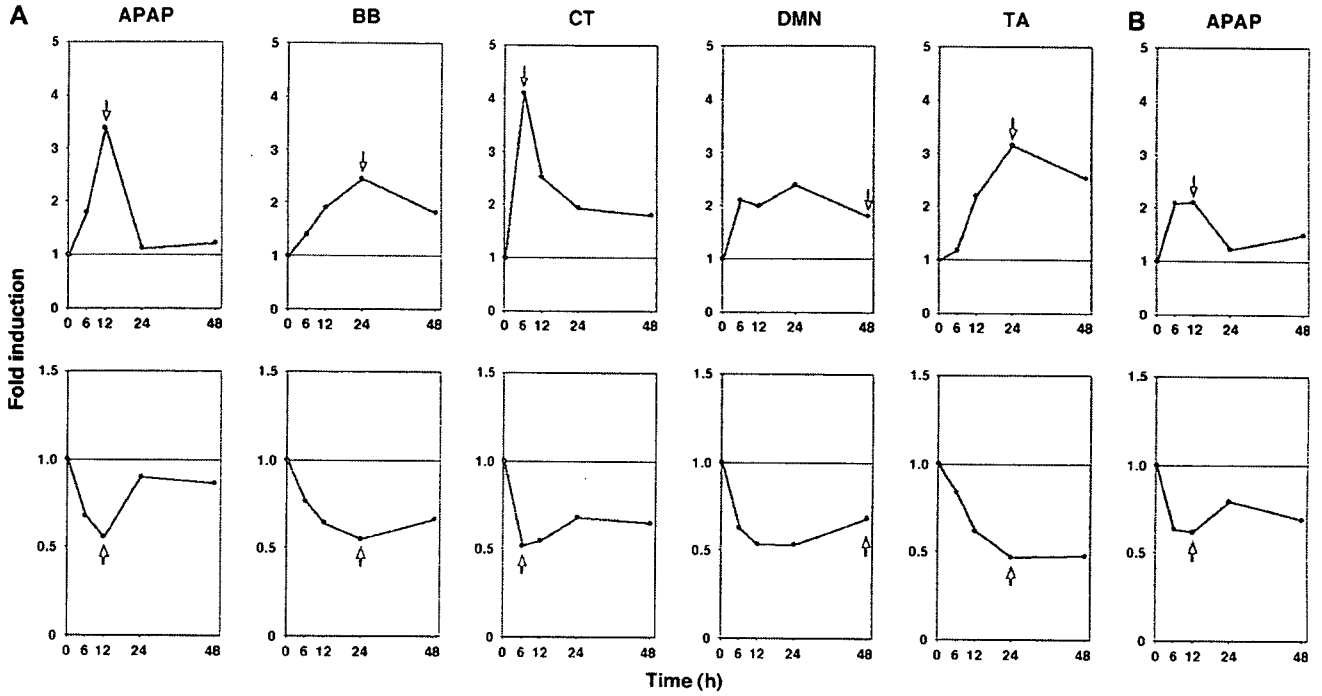

FIG. 4. QT clustering analysis of hepatic gene expression in rats administered the five chemicals. (A) The clustering setting for the correlation coefficient was 0.5 and contained more than 100 genes. The method for QT clustering analysis was described in Materials and Methods. Each figure shows an expression profile using the average of the clustered genes. Arrows indicate the maximal toxic time in each chemical-administered group estimated from the change of biochemical markers. In the upper group, the APAP, BB, CT, DMN, and TA clusters contained 109, 105, 143, 139, and 153 genes, respectively. In the lower group, the APAP, BB, CT, DMN, and TA clusters contained 122, 159, 180, 144, and 163 genes, respectively. (B) QT clustering analysis in APAP-administered rats performed using Agilent Rat cDNA microarray kit G4105A. The clustering setting for the correlation coefficient was 0.68 and contained more than 1,000 genes. The upper cluster contained 1,058 genes, and the lower cluster contained 1,106 genes.

Microarrays are now available that contain huge numbers of genes, even those whose functions are not clear, and the effects of a chemical on the gene expression cannot be assessed with a single microarray experiment.

In this study, we evaluated five typical hepatotoxic chemicals these were thought to cause zone-3 necrosis (Zimmerman, 1999). The dose levels of APAP (Price and Jollow, 1982; Sato and Izumi, 1989), BB (Chakrabarti and Brodeur, 1984), CT (Theocharis *et al.*, 2001), DMN (Asakura *et al.*, 1998), and TA (Wang *et al.*, 2000; Zaragoza *et al.*, 2000) were selected based on their association with detectable hepatotoxicity as previously reported. These data confirmed that the hepatotoxicity models of all the chemical-administered groups were successfully conducted, and the toxic time points of APAP, BB, CT, DMN, and TA were estimated as 12, 24, 6, 48, and 24 h, respectively. The maximal toxic times of BB (Chakrabarti and Brodeur, 1984), DMN (Asakura *et al.*, 1998), and TA (Wang *et al.*, 2000; Zaragoza *et al.*, 2000, respectively) in rats were the same as previously reported. In the CT-administered rats, AST and ALT elevated significantly at 6 and 48 h in the present study, but the CT toxicity assessed by serum AST and ALT increased at 6 to 24 h (AST) or 6 to 36 h (ALT) in a time-dependent manner, respectively (Zimmerman, 1999). In APAP-administered rats, AST and ALT elevated significantly at 6 and 12 h, but the serum AST and ALT were previously reported to be evaluated at 24 h by APAP administration (Hong *et al.*, 1992; Wang *et al.*, 1999). In the present study, the biochemical markers reflected the major gene expression profiles (Figs. 2, 3, 4, and 5).

We performed hierarchical clustering using gene groups whose expression levels were distinctively changed at the toxic time points (Fig. 1). At the maximal toxic time, CT and TA were sorted in a relatively close cluster. At the maximal toxic time, BB and DMN were sorted in a similar cluster. However, all APAP-administered groups were sorted in a different cluster. We performed many other types of hierarchical clustering by using other gene groups such as enzymes, signal transductions, and so on, and the results were almost the same as shown in Figure 1 (data not shown). Although studies concerning many hepatotoxicants including APAP, BB, CT, DMN, and TA administered to Sprague-Dawley rats have been reported (Kier *et al.*, 2004, McMillian *et al.*, 2004a,b), there has been no attempt of such a hierarchical clustering analysis using five chemicals. Thus, that the gene expression profiles of APAP administration were different from other those of the four chemicals constitutes new information.

In handling microarray data, it is necessary to consider what kinds of effects are relevant to the purpose of the experiments.

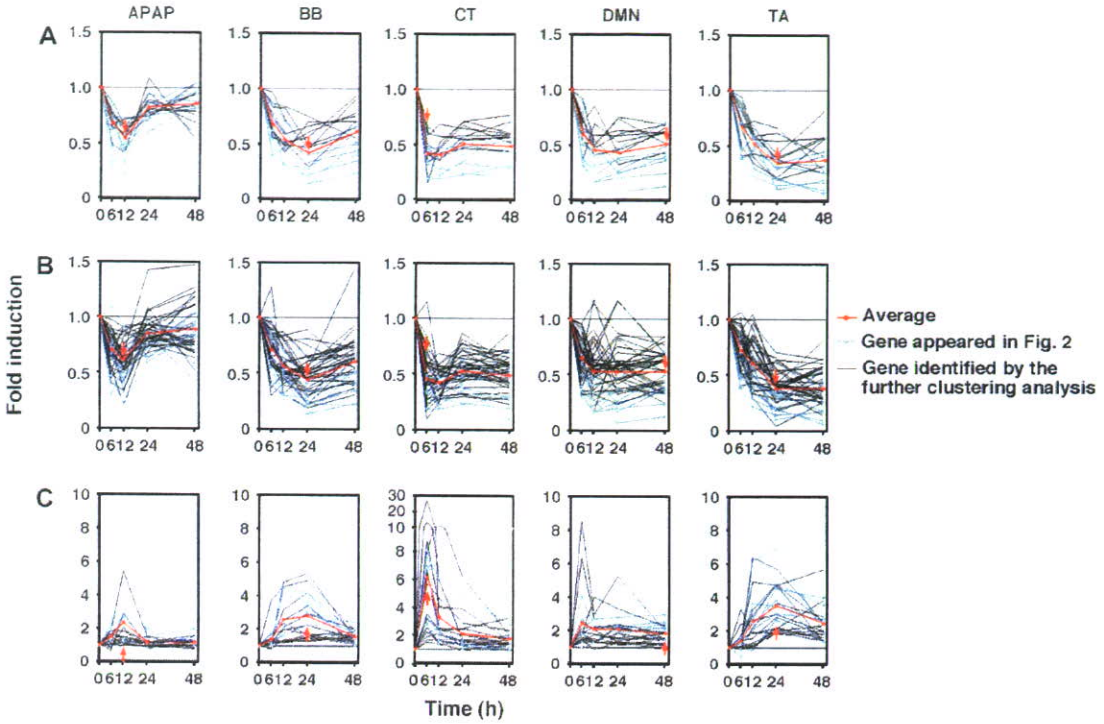

FIG. 5. Gene expression profiles of each group of chemical-administered rats identified by QT clustering analysis. The blue lines show the expression profiles of the genes that appeared in Figure 2. The red lines indicate the average of the expression. The red arrows indicate the maximal toxic time in each chemical-administered group estimated from the change of biochemical markers. (A) The expression profiles of genes down-regulated in the five chemical-administered groups. The expression profiles of genes that did not appear in Figure 2 are indicated by black lines. (B) The expression profiles of genes down-regulated in four of five chemical-administered groups. (C) The expression profiles of genes up-regulated in four of five chemical-administered groups. The expression profiles of the clustered genes that did not appear in Figure 2 are indicated by black lines. The analysis setting for the correlation coefficient was 0.65 and contained more than 10 genes.

We identified 20 representative genes whose up- or down-regulation peaks overlapped with the maximal toxic time (Fig. 2). In each of the chemical-administered rats, almost all genes identified in the present study showed similar expression profiles. The expression profile was confirmed in five representative genes, resulting in the overlapped profile with that of DNA microarray. Moreover, 17 of 20 genes were also identified by QT clustering analysis (Fig. 5). Data from QT clustering are independent of the hepatotoxicity estimated by serum biochemical markers. The present results showed the potential usefulness of 17 identified genes as toxicity markers. Most of the identified genes were not described previously as having a relationship with hepatotoxic chemicals. For example, TA administration up-regulated rat aldorase A mRNA (Bulera *et al.*, 2001). CtsL was up-regulated at the hepatic mRNA level after 24 h in BB- and TA-administered rats (Heijne *et al.*, 2003; Bulera *et al.*, 2001, respectively). Hmox1 was reported to be up-regulated by four chemicals, APAP (Chiu *et al.*, 2002), BB (Heijne *et al.*, 2003), CT (Montosi *et al.*, 1998), and TA (Bulera *et al.*, 2001; Matsuura *et al.*, 1988), in rats *in vivo*. In the present study, the expression of CYP2E1, which possibly catalyzes the induced toxicity of the five chemicals (Jeong, 1999; Lauriault *et al.*, 1992; Wang *et al.*, 2000; Zimmerman, 1999) was only slightly changed (data not shown), suggesting that the induction of CYP2E1 would not be involved.

QT clustering analysis is usually performed to determine the specific gene expression patterns. The resulting clusters gave us a good indication of the types of gene expression patterns that existed in the data (Heyer *et al.*, 1999). The gene expression patterns obtained from QT clustering analysis were major patterns expressed with each type of chemical administration (Fig. 4A). However, the extent of toxicity estimated by serum biochemical markers was different for each chemical. The average of each gene expression profile from QT clustering was overlapped with the changes of the serum biochemical markers. Furthermore, we performed QT clustering using Agilent Rat cDNA microarray kit G4105A in APAP-administered rat samples, the results of which showed almost the same expression profile (Fig. 4B). From this cDNA microarray, we confirmed the reproducibility of the new QT clustering data.

In conclusion, we identified 17 potential toxicity markers. It was not clarified whether all of the genes were related to the development of toxicity or whether these genes were related to each other. In the present study, we found that the expression profile analysis of the chemical administration could be used to estimate the maximal toxic time independently of the toxicity

grade. This expression profile analysis could also be a tool for identifying potential hepatotoxicants. This would be a new approach for determining hepatotoxicity by microarray analysis. We demonstrated that these two approaches, serum biochemical markers and two different QT clustering analyses, yielded the same results. For further studies, detailed time courses, multidose levels, and evaluation of other hepatotoxicants will be performed.

SUPPLEMENTARY DATA

Supplementary data are available online at www.toxsci.oxfordjournals.org.

ACKNOWLEDGMENTS

This work was supported in part by a grant from the Ministry of Education, Science, Sports, and Culture of Japan, and by Research on Advanced Medical Technology, Health and Labor Science Research Grants from the Ministry of Health, Labor and Welfare of Japan. We thank Mr. Brent Bell for reviewing the manuscript.

REFERENCES

Asakura, S., Daimon, H., Sawada, S., and Sagami, F. (1998). A short-term assessment of tumor-promotion activity in the livers of rats treated with two genotoxic methylating agents: Dimethylnitrosamine and methylnitrosourea. *Toxicol. Lett.* **98,** 155–167.

Bulera, S. J., Eddy, S. M., Ferguson, E., Jatkoe, T. A., Reindel, J. F., Bleavins, M. R., and De La Iglesia, F. A. (2001). RNA expression in the early characterization of hepatotoxicants in Wistar rats by high-density DNA microarrays. *Hepatology* **33,** 1239–1258.

Chakrabarti, S., and Brodeur, J. (1984). Dose-dependent metabolic excretion of bromobenzene and its possible relationship to hepatotoxicity in rats. *J. Toxicol. Environ. Health* **14,** 379–391.

Chiu, H., Brittingham, J. A., and Laskin, D. L. (2002). Differential induction of heme oxygenase-1 in macrophages and hepatocytes during acetaminophen-induced hepatotoxicity in the rat: Effects of hemin and biliverdin. *Toxicol. Appl. Pharmacol.* **181,** 106–115.

Dyroff, M. C., and Neal, R. A. (1981). Identification of the major protein adduct formed in rat liver after thioacetamide administration. *Cancer Res.* **41,** 3430–3435.

Heijne, W. H., Stierum, R. H., Slijper, M., van Bladeren, P. J., and van Ommen, B. (2003). Toxicogenomics of bromobenzene hepatotoxicity: A combined transcriptomics and proteomics approach. *Biochem. Pharmacol.* **65,** 857–875.

Heyer, L. J., Kruglyak, S., and Yooseph, S. (1999). Exploring expression data: Identification and analysis of coexpressed genes. *Genome Res.* **11,** 1106–1115.

Hong, R. W., Rounds, J. D., Helton, W. S., Robinson, M. K., and Wilmore, D. W. (1992). Glutamine preserves liver glutathione after lethal hepatic injury. *Ann. Surg.* **215,** 114–119.

Hughes, T. R., Mao, M., Jones, A. R., Burchard, J., Marton, M. J., Shannon, K. W., Lefkowitz, S. M., Ziman, M., Schelter, J. M., Meyer, M. R., *et al.* (2001). Expression profiling using microarrays fabricated by an ink-jet oligonucleotide synthesizer. *Nat. Biotech.* **19,** 342–347.

Hunter, A. L., Holscher, M. A., and Neal, R. A. (1977). Thioacetamide-induced hepatic necrosis. I. Involvement of the mixed-function oxidase enzyme system. *J. Pharmacol. Exp. Ther.* **200,** 439–448.

Jeong, H. G. (1999). Inhibition of cytochrome P450 2E1 expression by oleanolic acid: Hepatoprotective effects against carbon tetrachloride-induced hepatic injury. *Toxicol. Lett.* **105,** 215–222.

Kier, L. D., Neft, R., Tang, L., Suizu, R., Cook, T., Onsurez, K., Tiegler, K., Sakai, Y., Ortiz, M., Nolan, T., *et al.* (2004). Applications of microarrays with toxicologically relevant genes (tox genes) for the evaluation of chemical toxicants in Sprague Dawley rats *in vivo* and human hepatocytes *in vitro*. *Mutat. Res.* **549,** 101–113.

Lauriault, V. V., Khan, S., and O'Brien, P. J. (1992). Hepatocyte cytotoxicity induced by various hepatotoxins mediated by cytochrome P-450IIE1: Protection with diethyldithiocarbamate administration. *Chem. Biol. Interact.* **81,** 271–289.

Luo, L., Salunga, R. C., Guo, H., Bittner, A., Joy, K. C., Galindo, J. E., Xiao, H., Rogers, K. E., Wan, J. S., Jackson, M. R., *et al.* (1999). Gene expression profiles of laser-captured adjacent neuronal subtypes. *Nat. Med.* **5,** 117–122.

Matsuura, Y., Fukuda, T., Yoshida, T., and Kuroiwa, Y. (1988). Inhibitory effect of zinc-protoporphyrin on the induction of heme oxygenase and the associated decrease in cytochrome P-450 content in rats. *Toxicology* **50,** 169–180.

McMillian, M., Nie, A. Y., Parker, J. B., Leone, A., Bryant, S., Herlich, J., Yieh, L., Bittner, A., Liu, X., Wan, J., *et al.* (2004a). Inverse gene expression patterns for macrophage activating hepatotoxicants and peroxisome proliferators in rat liver. *Biochem. Pharmacol.* **67,** 2141–2165.

McMillian, M., Nie, A. Y., Parker, J. B., Leone, A., Bryant, S., Kemmerer, M., Herlich, J., Liu, Y., Yieh, L., Bittner, A., *et al.* (2004b). A gene expression signature for oxidant stress/reactive metabolites in rat liver. *Biochem Pharmacol.* **68,** 2249–2261.

Montosi, G., Garuti, C., Iannone, A., and Pietrangelo, A. (1998). Spatial and temporal dynamics of hepatic stellate cell activation during oxidant-stress-induced fibrogenesis. *Am. J. Pathol.* **152,** 1319–1326.

Price, V. F., and Jollow, D. J. (1982). Increased resistance of diabetic rats to acetaminophen-induced hepatotoxicity. *J. Pharmacol. Exp. Ther.* **220,** 504–513.

Sato, C., and Izumi, N. (1989). Mechanism of increased hepatotoxicity of acetaminophen by the simultaneous administration of caffeine in the rat. *J. Pharmacol. Exp. Ther.* **248,** 1243–1247.

Theocharis, S. E., Margeli, A. P., Skaltsas, S. D., Spiliopoulou, C. A., and Koutselinis, A. S. (2001). Induction of metallothionein in the liver of carbon tetrachloride intoxicated rats: An immunohistochemical study. *Toxicology* **161,** 129–138.

Wang, T., Shankar, K., Ronis, M. J., and Mehendale, H. M. (2000). Potentiation of thioacetamide liver injury in diabetic rats is due to induced CYP2E1. *J. Pharmacol. Exp. Ther.* **294,** 473–479.

Wang, P. Y., Kaneko, T., Wang, Y., and Sato, A. (1999). Acarbose alone or in combination with ethanol potentiates the hepatotoxicity of carbon tetrachloride and acetaminophen in rats. *Hepatology* **29,** 161–165.

Zaragoza, A., Andres, D., Sarrion, D., and Cascales, M. (2000). Potentiation of thioacetamide hepatotoxicity by phenobarbital pretreatment in rats. Inducibility of FAD monooxygenase system and age effect. *Chem. Biol. Interact.* **124,** 87–101.

Zimmerman, H. J. (1999). *Hepatotoxicity: The Adverse Effects of Drugs and Other Chemicals on the Liver,* 2nd ed., pp. 229–274. Lippncott Williams & Wilkins, Philadelphia.

Pharmacokinetics of Paclitaxel in Ovarian Cancer Patients and Genetic Polymorphisms of CYP2C8, CYP3A4, and MDR1

Miki Nakajima, PhD, Yuto Fujiki, MS, Satoru Kyo, MD, PhD, Taro Kanaya, MD, PhD, Mitsuhiro Nakamura, MD, Yoshiko Maida, MD, PhD, Masaaki Tanaka, MD, PhD, Masaki Inoue, MD, PhD, and Tsuyoshi Yokoi, PhD

Interindividual differences in the pharmacokinetics of paclitaxel and its metabolites in Japanese ovarian cancer patients were investigated in relation to genetic polymorphisms of the CYP2C8, CYP3A4, *and* MDR1 *genes. The area under the concentration-time curve (AUC) ratios of paclitaxel/6α-hydroxypaclitaxel and paclitaxel/3′-p-hydroxypaclitaxel calculated as the metabolic index of CYP2C8 and CYP3A4 showed 13- and 12-fold interindividual variations, respectively. No patient had any* CYP2C8 *variants, while 2 patients were heterozygotes of* CYP3A4*16. *For the* MDR1 *gene, the frequencies of –129C, 1236C, 2677T, 2677A, and 3435T alleles were 2.2%, 8.7%, 56.5%, 4.4%, and 52.2%, respectively. Subjects possessing the 3435T allele had a significantly (P < .05) higher AUC of 3′-p-hydroxypaclitaxel compared to those possessing the 3435C allele. Leukocytopenia was significantly (P < .05) related to the AUC of paclitaxel. Genotyping of the* CYP2C8, CYP3A4, *and* MDR1 *genes might not be essential to predict adverse effects of paclitaxel in Japanese patients, although an allelic variant of* MDR1 *may functionally affect the pharmacokinetics of its metabolite.*

Keywords: *Genetic polymorphism; cytochrome P450; P-glycoprotein; pharmacokinetics*
Journal of Clinical Pharmacology, 2005;45:674-682

Paclitaxel, a key drug for the chemotherapy of ovarian cancers, exerts its cytotoxic action through the promotion of microtubule assembly and stabilization by preventing depolymerization.[1] Combination therapy with paclitaxel and carboplatin, including monthly or weekly administration, is currently used as a standard protocol for the chemotherapy of ovarian cancers, both in adjuvant or neoadjuvant settings. In the standard protocol of this combination therapy, patients suffer from adverse effects specific to paclitaxel, including arthralgia, myalgia, and peripheral neuropathy, in addition to common toxicities such as nausea, vomiting, and alopecia. Particularly, the severity of the adverse effects remarkably varies among individual patients. One cause of this is undoubtedly variation in the plasma concentration of paclitaxel. Understanding of the interindividual difference in the pharmacokinetics of paclitaxel will therefore provide important information for the establishment of safe and effective protocols.

The primary route of elimination of paclitaxel is hepatic metabolism and biliary excretion.[2] Three metabolites of paclitaxel, 6α-hydroxypaclitaxiel, 3′-*p*-hydroxypaclitaxel, and 6α,3′-*p*-dihydroxypaclitaxel, have been detected in humans.[3-5] All 3 metabolites have been reported to be less potent than paclitaxel in inhibiting cell growth in vitro.[4,6] The metabolism of paclitaxel is catalyzed by cytochrome P450 (CYP) enzymes. The formation of 6α-hydroxypaclitaxel is catalyzed by CYP2C8,[3] whereas the formation of 3′-*p*-

From Drug Metabolism and Toxicology, Division of Pharmaceutical Sciences (Dr Nakajima, Ms Fujiki, Dr Yokoi), and the Department of Obstetrics and Gynecology, Graduate School of Medical Science (Dr Kyo, Dr Kanaya, Dr Nakamura, Dr Maida, Dr Tanaka, Dr Inoue), Kanazawa University, Kanazawa, Japan. Submitted for publication December 19, 2004; revised version accepted February 24, 2005. Address for reprints: Miki Nakajima, PhD, Drug Metabolism and Toxicology, Division of Pharmaceutical Sciences, Graduate School of Medical Science, Kanazawa University, Kakuma-machi, Kanazawa 920-1192, Japan.
DOI: 10.1177/0091270005276204

hydroxypaclitaxel is catalyzed by CYP3A4.[4,7] 6α,3′-*p*-Dihydroxypaclitaxel is formed by stepwise hydroxylations by CYP2C8 and CYP3A4. Since the ratio of 6α-hydroxypaclitaxel to 3′-*p*-hydroxypaclitaxel has been reported to be 6:1 in human bile,[8] CYP2C8 is the principal enzyme involved in the elimination and detoxification of paclitaxel. P-glycoprotein, an ATP-dependent efflux pump, is involved in limiting the absorption of xenobiotics from the gut lumen and in the biliary and urinary excretion of their substrates. Paclitaxel has been identified as a substrate of P-glycoprotein,[9,10] and the role of P-glycoprotein in paclitaxel resistance in tumors has also been proved.[11,12] Since P-glycoprotein is an important factor in the biliary excretion of many drugs, it might also possibly function in the biliary elimination of paclitaxel.

The prediction of adverse effects in individual patients is an important issue, as it would contribute to enhanced drug safety and efficacy. Functional genetic polymorphisms for drug-metabolizing enzymes and transporters are recognized as a critical factor influencing the pharmacokinetics of drugs.[13,14] Genetic polymorphisms in the *CYP2C8*, *CYP3A4*, and *MDR1* genes have been reported, which may affect the pharmacokinetics of paclitaxel. However, no information is available on the effects of such genetic polymorphisms on the pharmacokinetics of paclitaxel in vivo. Such a background prompted us to investigate the interindividual variability of the pharmacokinetics of paclitaxel and its metabolites in ovarian cancer patients in relation to genetic polymorphisms of the *CYP2C8*, *CYP3A4*, and *MDR1* genes.

MATERIALS AND METHODS

Materials

Paclitaxel was kindly provided by Bristol-Myers Squibb Pharmaceutical (Tokyo, Japan). 6α-Hydroxypaclitaxel and 3′-*p*-hydroxypaclitaxel were purchased from Daiichi Pure Chemicals (Tokyo, Japan). Docetaxel (Taxotere) was obtained from Aventis Pharma (Tokyo, Japan). The Puregene DNA isolation kit was from Gentra Systems (Minneapolis, Minn). Taq DNA polymerase was from Greiner Japan (Tokyo, Japan). Restriction enzymes were purchased from Toyobo (Osaka, Japan), Takara (Kyoto, Japan), or New England Biolabs (Beverly, Mass). All other reagents were of the highest grade commercially available.

Patients, Drug Administration, and Blood Collection

This study was approved by the Ethics Committees of Kanazawa University and Kanazawa University Hospital. Written informed consent was obtained from 23 female patients (age: 54.9 ± 12.6 years [range, 23-74 years], body surface area: 1.53 ± 0.09 m^2 [range, 1.38-1.69 m^2]) with ovarian cancer. No patient had evidence of major alterations in hepatic, renal, or cardiac function at the time of the study. Paclitaxel (Taxol; Bristol-Myers Squibb, Tokyo, Japan) was administered as a 3-hour intravenous (IV) infusion at a dose of 180 mg/m^2 following premedication with dexamethasone (20 mg IV), diphenhydramine (50 mg orally), and famotidine (20 mg IV) for prophylaxis against hypersensitivity reactions. Thirty minutes after the end of the infusion of paclitaxel, carboplatin (Paraplatin, Bristol-Myers Squibb) was administered as a 1-hour infusion. The dose of carboplatin was calculated using the Chatelut formula, and the target area under the concentration-time curve (AUC) was 5 mg•min/mL. Granulocyte colony-stimulating factor was administered when the neutrophil count was <1000/mm^3. Blood samples (5 mL) were obtained from a cubital vein opposite the infusion site, before the infusion of paclitaxel, at the middle and the end of infusion, and 1, 2, 3, 8, 16, and 24 hours after the end of infusion. Blood samples were centrifuged to collect the plasma. The plasma samples were stored at –20°C until the analyses.

Sample Processing and High-Performance Liquid Chromatography Analysis

The concentrations of paclitaxel and its metabolites in plasma were determined by high-performance liquid chromatography (HPLC) with solid-phase extraction according to the method of Willey et al,[15] with slight modifications. LiChrolut CN columns (1 mL, 200 mg; Merck, Darmstadt, Germany) were first conditioned with 2 mL of methanol followed by 2 mL of 0.01 M ammonium acetate buffer (pH 5.0). To the plasma samples (0.5 mL), 0.5 mL of 0.2 M ammonium acetate buffer (pH 5.0) and docetaxel (100 ng) as an internal standard were added. The samples were loaded onto the columns and washed with 2 mL of 0.01 M ammonium acetate buffer (pH 5.0), 1 mL of 20% methanol in 0.01 M ammonium acetate buffer (pH 5.0), and 1 mL of hexane. The columns were dried under vacuum for 1 minute. The analytes were eluted from the columns with 2 mL of 0.1% triethylamine in acetonitrile. The eluent was